Polymer modeling suggests correlations between chromatin phase separation and nuclear shape fluctuations

Ali Goktug Attar[1], Jaroslaw Paturej[2], Edward J. Banigan[3,*], and Aykut Erbas[1,2,*]

1. UNAM-National Nanotechnology Research Center and Institute of Materials Science & Nanotechnology, Bilkent University, Ankara 06800, Turkey

2. Institute of Physics, University of Silesia, Chorzów, 41-500, Poland

3. Institute for Medical Engineering and Science and Department of Physics, Massachusetts Institute of Technology, Cambridge, MA 02139, USA

KEYWORDS Molecular shell, nuclear rigidity, phase separation, chromosomes, coarse-grained modeling

---

ABSTRACT: Abnormalities in the shapes of mammalian cell nuclei are common hallmarks of a variety of diseases, including progeria, muscular dystrophy, and various cancers. Experiments have shown that there is a causal relationship between chromatin organization and nuclear morphology. Decreases in heterochromatin levels, perturbations to heterochromatin organization, or increases in euchromatin levels all lead to nuclear bleb formation and nuclear rupture. However, the polymer physical mechanisms of how chromatin governs nuclear shape and integrity are poorly understood. To investigate how hetero- and euchromatin, which are thought to microphase separate *in vivo*, govern nuclear morphology, we implemented a composite coarse-grained polymer and elastic-shell model. By varying chromatin volume fraction (density), heterochromatin structure and levels, and heterochromatin-lamina interactions, we show how the spatial organization of chromatin polymer phases within the nucleus could perturb nuclear shape in some scenarios. Increasing the volume fraction of chromatin in the cell nucleus stabilizes the nuclear lamina against large fluctuations. However, surprisingly, we find that increasing heterochromatin levels or heterochromatin-lamina interactions enhances nuclear shape fluctuations in our simulations. In contrast, shape fluctuations are largely insensitive to the internal organization of the heterochromatin, such as the presence or absence of chromatin-chromatin crosslinks. Increasing the stiffness of the lamina suppresses the effects of heterochromatin on envelope fluctuations. Therefore, our simulations suggest that heterochromatin accumulation at the nuclear periphery could perturb nuclear morphology in a nucleus or nuclear region that is sufficiently soft, while chromatin could stabilize a nucleus through mechanisms other than chromatin microphase organization if the lamina is stiff.

Introduction

The mammalian genome confined inside the ~10 μm nucleus is composed of multiple extremely long DNA polymer chains, referred to as chromosomes. Chromosomes are packaged heterogeneously into chromatin fibers through a set of structural and functional DNA-associating proteins. These chromatin fibers are dynamically organized into polymer phases[1–5], generally known as euchromatin and heterochromatin. The spatial organization of chromatin is essential for regulating vital biological processes[6–8], such as transcription, replication, and differentiation. Perturbations and alterations to chromatin organization are associated with a variety of human diseases and conditions, including aging, progeria, muscular dystrophy, and various cancers[9–12]. Abnormal nuclear morphology has long been used as a hallmark of these conditions, but recent research has shown that there are mechanistic links between alterations to nuclear architecture and perturbations to nuclear function. Recent experiments have also established that perturbed chromatin organization is causally connected to disruptions in nuclear shape[13–17], suggesting another intriguing link between chromatin spatial organization and nuclear function. Nonetheless, the physical mechanisms through which chromatin governs nuclear shape are not fully explained, and it is unclear whether and how the overall (micro)phase organization of chromatin contributes to nuclear morphology.

Chromatin has two main types, euchromatin, and heterochromatin, which are distinguished mainly by their transcriptional activities, compaction, and organization. Euchromatin is transcriptionally active and maintains an open, accessible structure. Heterochromatin is composed of compacted chromatin domains in which transcriptional activity is low and chromatin is generally inaccessible. Regions of heterochromatin are further classified as facultative and constitutive, depending on the histone modifications they contain. In conventional nuclear chromatin organization, heterochromatin-rich regions of chromatin are predominantly located at the nuclear periphery, beneath the nuclear lamina, whereas the euchromatin is generally located in the nuclear interior[18]. Various measurement techniques, ranging from whole-nucleus micromanipulatio[14,19,20] to nuclear elastography calculations indicate that nuclear heterochromatin has a larger elastic modulus than euchromatin[21]. The heterochromatin fiber seems to have a longer persistence length (i.e., distance below which a polymer behaves like a rod) than euchromatin[22], and this difference may influence chromatin organization via entropic effect[23,24]. Additionally, heterochromatin is thought to exhibit stronger self-attraction than euchromatin[1,5], which can result in a mesoscale phase separation of chromatin within the nucleus[3,4,25].

Chromatin phase separation, in turn, is thought to spatially organize chromatin within the confines of the nucleus, which may deform in response to this internal organization. Treatment of nuclei with drugs that inhibit enzymes that alter histone modifications (e.g., deacetylases, demethylases, and methyltransferases),

can either induce or inhibit the formation of shape abnormalities known as nuclear "blebs"[14]. These deformations are chromatin-filled protrusions that frequently rupture and correlate with increased DNA damage[26,27], as well as various diseases[28,29]. Inhibition of deacetylases or methyltransferases increases euchromatic histone marks and increases nuclear blebbing, while inhibition of demethylases increases heterochromatin content and rescues nuclear shape[14,27]. Similarly, the loss of heterochromatin protein 1α (HP1α), a chromatin crosslinker protein that can induce heterochromatin phase separation *in vitro*[30,31], induces nuclear bleb formation[32]. Despite these observations, it is unclear whether such alterations to chromatin phase organization are directly responsible for blebbing.

Beyond localized shape disruptions, the spatial distribution of heterochromatin and euchromatin may influence the shape of the entire nucleus. Immunostaining experiments in mouse rod cells have shown that reorganization and repositioning of heterochromatin to the nuclear interior coincide with a change from a prolate ellipsoidal shape to circular disc-like nuclear morphology[33]. Similarly, loss of peripheral heterochromatin in Hutchinson Gilford Progeria Syndrome (HGPS) patient cell[34,35] and aging *C. elegans* cell[36] leads to widespread wrinkling and folding of the nuclear envelope. Moreover, in HGPS cells, these shape changes can be reversed by heterochromatin compaction[14,27]. Hence, several lines of experimental evidence suggest that the 3D chromatin organization within the nucleus can affect global nuclear morphology.

Chromatin is further organized by interactions with the nuclear envelope. Chromatin may be localized to the envelope (e.g., to the lamina and embedded proteins) via lamins and other chromatin-tethering proteins or histone modifications and histone-modifying enzyme[33,37–39]. Any breakdown in this interaction mechanism can also affect the 3D chromatin organization and, in turn, nuclear morphology[13,37]. For example, the knockdown of a chromatin-tethering protein, PRR14, led to a wrinkled nuclear morphology with large undulations on the nuclear surface[40]. Furthermore, in *S. pombe*, knockouts of chromatin-tethering LEM domain proteins exhibited reduced nuclear stiffness and increased nuclear deformations, apparently due to loss of chromatin interactions with the nuclear envelope[41]. Together, these experiments suggest that robust chromatin interactions with the nuclear periphery are important for the maintenance of regular nuclear morphology.

Previous polymer modeling studies suggest that chromatin phase separation, chromatin-lamina interactions, and the chromatin volume fraction all can contribute to nuclear architecture[3,4,42,43] . Within a rigid boundary, competition between heterochromatin-driven phase separation and adsorption of heterochromatin to the lamina can control the spatial distributions of chromatin[4] , as well as its subtypes, hetero-, and euchromatin[5]. However, it is unclear whether these effects would be coupled to the morphology of a deformable polymeric

shell, such as the lamina. Elastic shell models confining simple homopolymers have shown that chromatin compaction/stiffness can aid in resisting nuclear deformations[19,32,44]. However, simulations of a similar model have suggested that chromatin-lamina interactions can destabilize nuclear shape in some scenarios[45]. Thus, the mechanisms through which chromosomes, considered as multiblock copolymers, may govern nuclear morphology have not been explored systematically.

To investigate the connection between chromatin organization and nuclear morphology, we use molecular dynamics (MD) to simulate heterochromatin phase separation confined inside of a polymeric shell representing the nuclear lamina. Focusing on a model in which the nuclear lamina is relatively soft, we find that heterochromatin self-interactions and heterochromatin's interactions with the nuclear lamina can cooperatively contribute to nuclear shape fluctuations. Our simulations show that the volume fraction of the chromosome polymers determines the strength of the effect of heterochromatin phase separation on nuclear morphological fluctuations. In addition, the interaction affinity of heterochromatin to the nuclear shell drastically influences nuclear morphology, resulting in distorted nuclear shapes. Strikingly, our results differ from the conventional picture of chromatin-driven nuclear morphology, in which heterochromatin, especially at the nuclear periphery, stabilizes nuclear shape. Nonetheless, our results are consistent with some experimental scenarios and suggest a new mechanism by which chromatin phase organization may govern nuclear morphology. Overall, our findings suggest that the physics of polymer mixtures and phase separation can explain aspects of chromatin-related nuclear morphology alterations.

Method

Molecular model of mammalian cell nucleus

Our genome model is represented by 8 self-avoiding coarse-grained Kremer-Grest[46] bead-spring triblock copolymers in implicit solvent (Figure 1A). These block copolymers model chromosomes as composed of self-interacting compartments extracted from high-throughput chromosome conformation capture (Hi-C) data from mouse rod cells[5]. Four of the eight block copolymers in our model are figured based on chromosome 1, while the other four are derived from chromosome 2. Each block copolymer is composed of 6002 beads. The 1000 beads at one end of each block polymer are assigned as constitutive heterochromatin, and the remaining 5000 beads represent genomic loci that can form A- or B-type compartments[5], generally corresponding to euchromatin and heterochromatin. Two additional beads are added to each end of the polymer chain to represent the telomeres. Each bead in the polymer chains represents 40 kilobase pairs (kb) of chromatin, and each bead has size $b = 1\sigma$, where σ is the unit length scale in the simulations. This resolution allows the construction of genomic contact maps comparable to Hi-C experiments studying chromatin compartmentalization[47–49]. In the simulations, the polymers are initially placed at random positions in a compact form[50] near the center of the spherical volume within the

shell (Figure 1A). The adjacent polymer beads are connected by non-extensible bond potentials, not allowing any bond crossing (See text for further details of the polymer model).

The beads composing the confining shell take care of the elasticity of the nucleus arising due to the lamin meshwork. In the initial preparation of the shell, each shell bead is randomly placed on the surface of a sphere, which has radius $R_0=42\sigma$. The beads are connected by non-extensible bond potentials. On average, each shell bead forms n_{bond} bonds to neighboring shell beads, with $5 \leq n_{\text{bond}} \leq 8$. These bonds are initially assigned by the predefined distance parameter such that they bond with nearest neighbors and prevent void spaces on the shell surface (Figure 1A). Throughout the simulation, the total numbers of bonds and beads are constant.

MD simulation parameters

The steric interactions between bonded and non-bonded beads are modeled by the Lennard-Jones (LJ) potential with various cut-off distances (see the Supplementary text for further simulation parameters). All simulations are run using LAMMPS MD package[51]. The simulation timestep is $\Delta t = 0.005\tau$, where τ is the unit time scale in the simulations and is equivalent to 200 MD steps. The minimization simulations are run for $3\text{x}10^4$ MD steps to allow for the initial relaxation of the shell. During the minimization simulations, the shell is shrunk to ≈90% of its initial volume as the assigned bonds reach their equilibrium length. The purpose of these simulations is local equilibration of shell structure and to reduce holes on the shell surface that could lead to chromatin escaping. Following, an additional 10^5 MD steps are run to relax the polymer blocks composing the initial model chromatid structures (Figure 1A). During the relaxation simulations, the attractive interaction between heterochromatin beads (i.e., constitutive and facultative heterochromatin and telomeres) and shell beads is switched on. Following, we run data production simulations to obtain a conventional nuclear organization with the interaction parameters listed in the Supplementary Information. The conventional nucleus simulations are run for $5\text{x}10^6$ MD timesteps to obtain a quasi-equilibrium chromatin distribution (Figure 1B). After recapitulating the conventional nuclei, we turned off the interactions between heterochromatic polymer subunits and the shell to recapitulate the inverted nuclei. The inverted nucleus simulations are run for 10^7 MD timesteps. The number of simulation steps for equilibration in conventional and inverted nucleus simulations is identified by the radial distribution and density plots (Figure S1 & Figure 1B). The polymer volume fraction φ is varied by decreasing the initial number of polymer blocks from n_{block}=8 to n_{block}=6 and n_{block}=4 to obtain φ=19% and φ=14%, respectively, in addition to the default value of φ=23%.

Calculation of nuclear shape fluctuations

To calculate nuclear shape fluctuations, we use the Fast Fourier Transform algorithm (FFT)[44,52]. At each timestep of data production simulations, we consider a thin slice of the shell with a width of $w=1\sigma$. For each bead in the slice, we calculate its displacement from the average radius of the slice (Figure 1C). We run the FFT algorithm on the obtained radial distances for the lowest 230 modes, q, and take the time average of the fluctuation amplitudes by considering only the last half of the simulation durations. We also measure the time-averaged standard deviation of the displacement from the mean radial position to quantify the dynamic fluctuations.

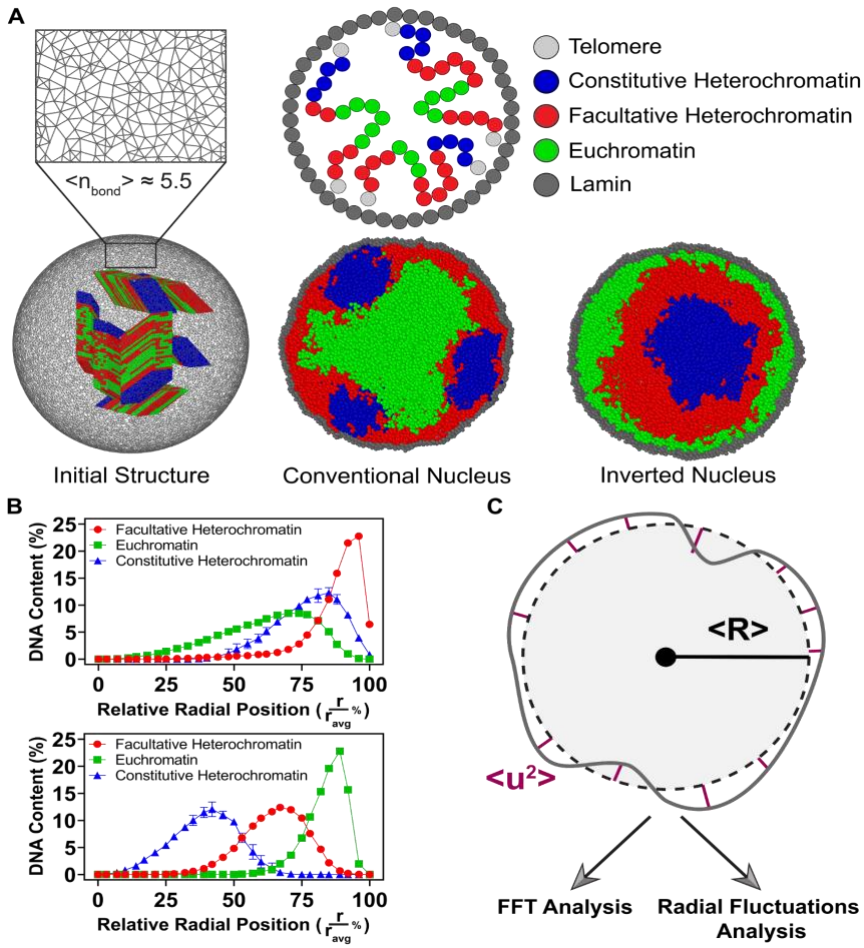

Figure 1: *A) Schematic illustration of the MD simulation model, with block copolymer and shell structures. Chromosome-like structures composed of 8 tri-block polymers are confined randomly inside the shell. Initial structures were run sequentially to obtain conventional and inverted nuclei. B) The density profiles of the different polymeric blocks in our simulations in conventional and inverted nuclei after relaxation. C) A schematic illustration of the analysis and metrics used to quantify nuclear shape fluctuations.*

Results

Higher Polymer Volume Fraction Suppresses Nuclear Shape Fluctuations

Recent studies suggest that chromatin density can influence the size and shape of the nucleus via entropic pressure of chromatin[53–55]. In parallel, chromatin decompaction was shown to increase nuclear size[56] and induce chromatin-filled protrusions known as nuclear bleb[16]. Conversely, hyperosmotic shock, which collapses chromatin, results in alterations to nuclear architecture[57].

Therefore, to understand the interplay between chromatin organization and nuclear shape, we performed simulations in which we varied the volume fraction chromatin polymers confined inside the elastic, deformable shell representing the lamina (see Methods). In our simulations, we considered scenarios for nuclear organization cases: conventional organization with heterochromatin at the periphery and euchromatin in the interior and "inverted" organization with heterochromatin in the interior and euchromatin at the periphery (Figure 2)[5,33]**.** The conventional chromatin distribution models many cells in which heterochromatin is preferentially located near the nuclear periphery, while the inverted organization serves as the limiting case in which peripheral heterochromatin levels vanish (Figure 1A).

In simulations, characterized nuclear shape fluctuations by calculating the deviations of the simulated structure from a sphere. To this end, we computed the Fourier spectrum of fluctuation modes as well as the root-mean-square (RMS) deviation of the elastic shell radius from a sphere with a constant mean radius[36,41,58] (see Methods). Our analyses show that decreasing the chromatin volume fraction increases the amplitudes of nuclear shape fluctuations, particularly at small wavenumbers, q, corresponding to length scales on the order of nuclear radius (Figure 2A). Thus, chromatin volume fraction has a global effect on nuclear morphology, likely due to the ability of higher volume fractions to stabilize nuclear shape through polymer osmotic pressure.

Nuclear shape fluctuations are insensitive to the internal structure of heterochromatin

Across all volume fractions, we observed that the nucleus with conventional chromatin organization exhibits systematically higher fluctuation amplitudes and RMS shape fluctuations as compared to inverted nuclei (i.e., 40% higher fluctuations at the lowest volume fraction, φ=14%,) (Figure 2A,C). This contrasted with the idea that peripheral heterochromatin stabilizes nuclear morphology, so we next investigated whether these effects could be modulated by altering the internal structure of heterochromatin, which may be facilitated by alterations to histone modifications or chromatin-binding proteins, such as HP1[32].

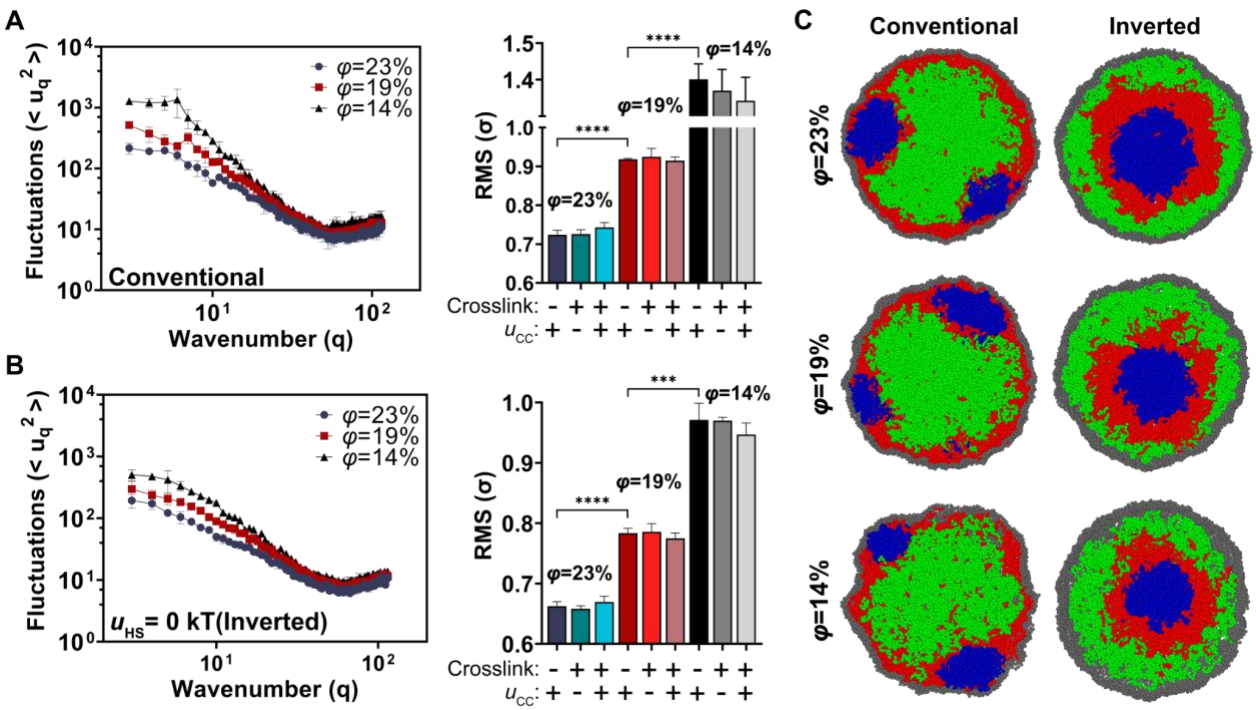

Figure 2: The effect of polymer volume fraction on nuclear shape fluctuations on conventional and inverted nuclei. *A) Shape fluctuation analysis was conducted on simulations at various volume fractions for conventional nuclei at three different volume fractions (φ=14%, φ=19%, and φ=23%). The constitutive heterochromatin domains (blue) are crosslinked or not and the LJ potential, u_{CC}, between constitutive heterochromatin beads, is switched on and off, as indicated by +/- beneath each bar in the bar plot at right. B) The Fourier spectrum of fluctuations and the RMS amplitudes plotted for inverted simulations. C) Representative snapshots of chromatin spatial organization and nuclear morphology in conventional and inverted scenarios for different chromatin volume fractions*

Our standard chromatin model consisted of constitutive heterochromatin beads that had nonspecific attractive interactions with each other. In addition to this model, we tested whether intra-domain linkages between constitutive heterochromatin beads (i.e., chromatin-chromatin crosslinks) could alter nuclear shape fluctuations. For this model, constitutive heterochromatin beads were permanently crosslinked to each other by bonds similar to those connecting polymer chains.

We performed simulations at each of the three different volume fractions with and without constitutive heterochromatin crosslinking and with or without nonspecific attractive constitutive heterochromatin-constitutive heterochromatin attractions (Figure 2). Simulations showed that the absence of crosslinking influences heterochromatin spatial organization in conventional nuclei; constitutive heterochromatin

domains tended to merge (SI text Figure S3). However, the distribution of constitutive heterochromatin domains did not alter the shape fluctuations, as measured by either the Fourier spectrum or the RMS shape fluctuations of the shell (Figure 2). The presence or absence of crosslinking also did not change shape fluctuations in the inverted nucleus cases. Similarly, we observed that the shape fluctuations were insensitive to the presence or absence of nonspecific heterochromatin self-attraction, provided that intra-domain crosslinks were present. Altogether, this indicates that heterochromatin's spatial positioning, but not necessarily its internal structure, is critical in determining the level of shape fluctuations of the confining elastic shell.

Interactions between Heterochromatin and Shell Alter Nuclear Shape Fluctuations

Experiments have shown that heterochromatin-lamina interactions are critical in regulating nuclear morphology[40,59–61]. We model these interactions through a nonspecific (nonbonded) attractive interaction, with strength, u_{HS}, between heterochromatin and lamina shell beads. By varying u_{HS}, we investigated how heterochromatin-lamina interactions may regulate nuclear shape fluctuations, perhaps through variations in levels or interactions with chromatin-lamina tethering proteins, such as LBR[33,62,63] are altered. Our analysis reveals that increasing the strength of the heterochromatin-shell attraction significantly increases nuclear shape fluctuations regardless of the chromatin volume fraction (Figure 3A-C and SI text Figure S4). For systems with strong heterochromatin attractions, we observe large bulges and localized wrinkles on the shell (right column of Figure 3C). With strong interaction energies, although the radial chromatin organization is preserved, the heterochromatin domains distort the shell by wrapping it around the surface of the domain (Figure 3C). At the strongest attraction energy studied (u_{HS}=3kT), shape fluctuations increase drastically across all length scales (Figure 3A). Decreasing the attraction affinity from our standard value, u_{HS}=0.75 kT, to a lower value, u_{HS}=0.375 kT, reduces nuclear shape fluctuations, particularly in the small-wavenumber (large lengthscale) regime (Figure 3A).

However, in this scenario, the spatial organization of chromatin is altered. Facultative heterochromatin near the nuclear periphery is reduced, forming mesoscale, phase-separating heterochromatin domains (Figure 3A). When heterochromatin-shell interactions are set to u_{HS}= 0, which is the case of inverted nuclei, morphological fluctuations on even the smallest length scales (largest q) become much weaker (SI text Figure S4). The finding that chromatin-shell interactions can enhance nuclear shape fluctuations ran counter to our expectation that such interactions would stabilize nuclear shape, as they generally do *in vivo*[13,40,41]. We therefore tested whether this phenomenon is sensitive to the stiffness of the shell. In simulations with stiffer bonds between shell beads (effectively, a higher bending rigidity[44]), we found that the destabilizing effect of heterochromatin-shell interactions is weakened, albeit decreasing in high volume fractions (SI text

Figure S21). Altogether, our results suggest that attractive heterochromatin-shell interactions can enhance nuclear shape fluctuations under conditions with a sufficiently soft confining shell.

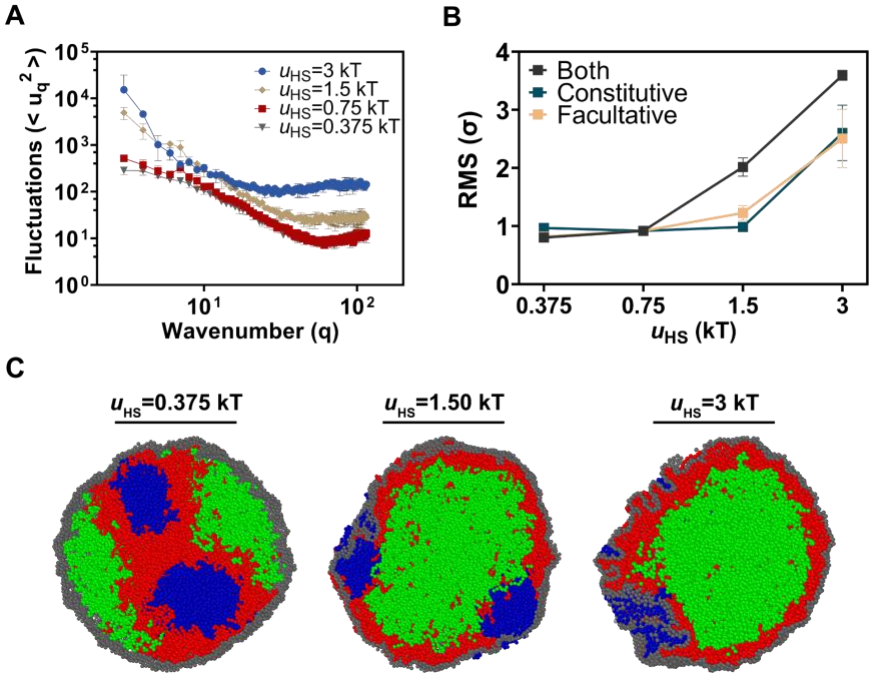

Figure 3: Heterochromatin-shell interactions influence nuclear shape fluctuations and morphology. *A) Nuclear shape fluctuations were calculated while the interaction between both heterochromatin types and the shell was altered in conventional nucleus simulations. The inverted nucleus simulations were run using the final state of the conventional nucleus simulations, and pairwise interactions between heterochromatic parts and the shell were subsequently abolished. The volume fraction was set to φ=19%. B) RMS nuclear shape fluctuations in three different scenarios of heterochromatin-shell interactions: one in which only constitutive heterochromatin is attracted to the shell, one in which only facultative heterochromatin is attracted to the shell, and one in which both types of heterochromatin are attracted to the shell. D) Snapshots of simulations from three different strengths of heterochromatin-shell interactions, where both heterochromatin types interaction are attracted to the lamina.*

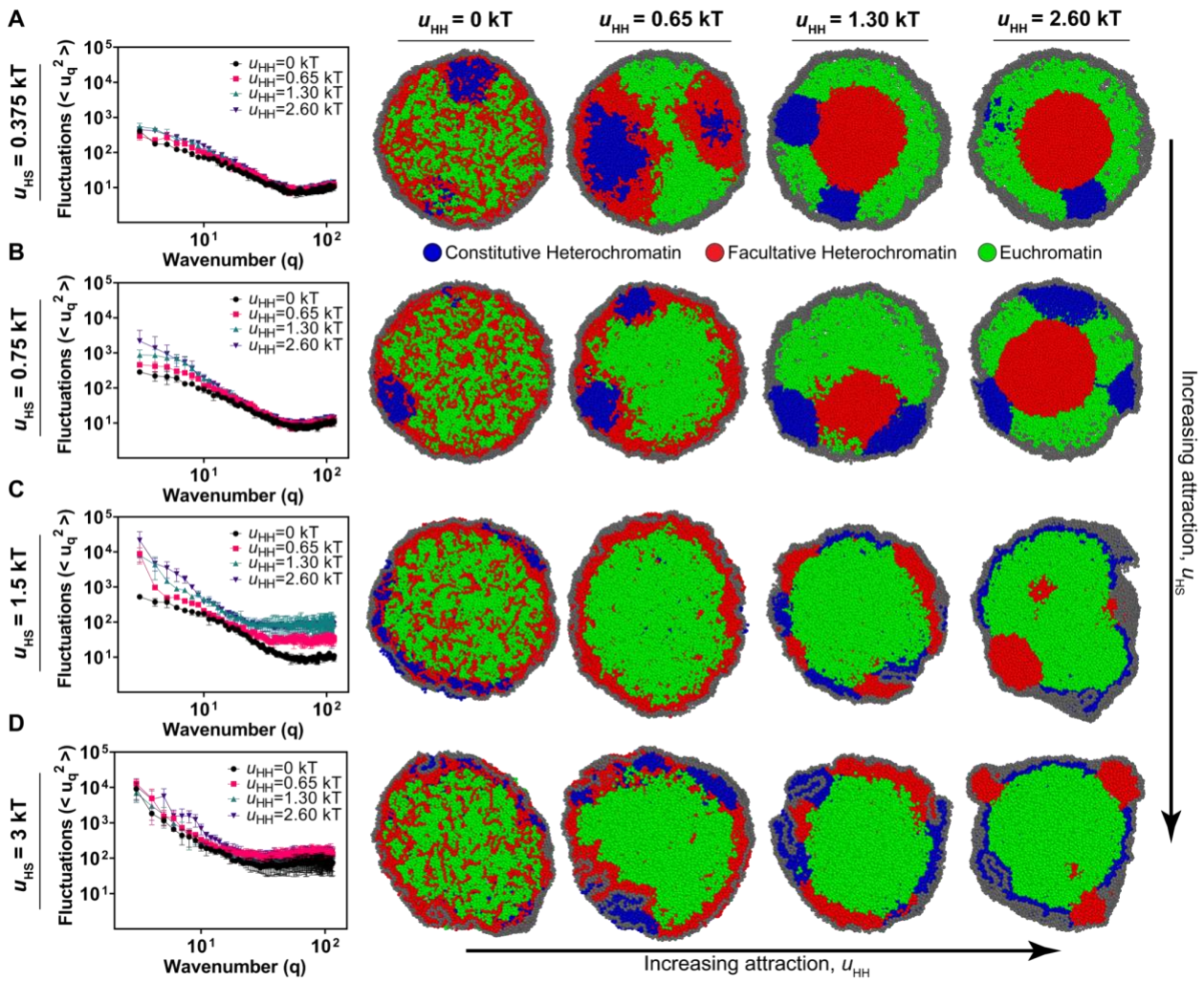

Figure 4. The interplay between heterochromatin-heterochromatin and heterochromatin-shell interactions. *A-D) Fourier spectra of nuclear shape fluctuations and corresponding snapshots for different self-affinities of heterochromatin (different for different colors in each plot and increasing from left to right across each row) and different heterochromatin-shell interactions strengths (increasing from top row to bottom row). A) The attraction affinities between facultative heterochromatin domains are varied, and the shell is set to u_{HS}=0.375kT. The polymer volume fraction is set to φ=19%. B) The attraction affinity between shell and heterochromatin domains is set to u_{HS}=0.75kT. C) The attraction affinity between shell and heterochromatin domains is set to u_{HS}=1.5kT. D) The attraction affinity between shell and heterochromatin domains is set to u_{HS}=3kT.*

Since the chromatin polymer in our simulations is composed of two types of heterochromatin, constitutive and facultative, we separately vary their interactions with the confining polymeric shell (Figure 3B). We find that increasing the strength of either type of chromatin with the lamina is sufficient to influence the

nuclear shape fluctuations (Figure 3B). Nevertheless, increasing only the facultative heterochromatin interactions with the shell causes the facultative heterochromatin to coat the inner surface of the shell completely by replacing the constitutive heterochromatin with a weaker interaction. The same mechanism does not appear with the constitutive heterochromatin due to strong heterochromatin-heterochromatin interactions collapsing these chromatin domains (SI text Figure S8).

On top of these changes, nuclear morphology for each perturbation is governed by the chromatin volume fraction. Strong shape fluctuations are further strengthened by lower chromatin volume fractions (SI text Figure S4-S9). Together, these findings indicate that the nuclear shape fluctuations can be affected by both heterochromatin types but via different mechanisms in the model.

Heterochromatin self-affinity alters its spatial distribution together with nuclear shape fluctuations

Since changes to heterochromatin-lamina interactions also produce alterations to the spatial distribution of heterochromatin, we sought a complementary method to probe whether the spatial distribution of heterochromatin can perturb nuclear shape fluctuations. Therefore, we studied the effects of changing the self-affinity of heterochromatic regions, as might occur when alterations are made to histone modifications.

Our simulations show that the strength of heterochromatin self-affinity can alter both the spatial distribution of chromatin and nuclear shape fluctuations. This is exemplified in Figure 4, where from left to right, heterochromatin-heterochromatin attractions increase, and from top to bottom heterochromatin-shell interactions increase. Abolishing the self-affinity of the facultative heterochromatin monomers (i.e., u_{HH}=0, left column of snapshots in Figure 4) decreases peripheral heterochromatin levels. Facultative heterochromatin beads coat the interior of the lamina, but additional heterochromatin has no preference for the nuclear periphery, and thus, disperse throughout the nuclear interior.

Peripheral organization of heterochromatin can also be disrupted by increasing the self-affinity of facultative heterochromatin to values larger than the chromatin-lamina attraction strength, i.e., $u_{HH} > u_{HS} > 0$ (Figure 4A-B, right). In this case, facultative heterochromatin forms a phase-separated region at the center of the nucleus, much like an inverted nucleus, as observed in a previous study[5]. Constitutive heterochromatin, in contrast, remains at the periphery since its self-affinity is unchanged in these simulations. Interestingly, this large-scale reorganization of heterochromatin positioning does not dramatically alter the shape fluctuations when chromatin-lamina interactions are weak (Figure 4, top two rows). Thus, there is only a modest difference between the shape fluctuations of conventional and inverted nuclei in this scenario.

Since we observe stronger shape fluctuations in simulations with strong chromatin-lamina interactions, we hypothesized that interactions with the densely packed peripheral heterochromatin layer beneath the shell surface could drive shape fluctuations (Figure 4A). Increasing the chromatin-lamina attraction strength leads to strong adsorption of heterochromatin to the interior of the lamina shell (Figure 4B-D). With strong chromatin-lamina interactions, even when the heterochromatin self-affinity is nonexistent (u_{HH}=0), a peripheral heterochromatin layer forms near the shell's interior surface and distorts the shell, increasing nuclear shape fluctuations (Figure 4D, leftmost image). Interestingly, if the heterochromatin-shell attraction is nonzero, heterochromatin further accumulates near the periphery further. In turn, this heterochromatin accumulation can further increase nuclear shape fluctuations (Figure 4B-D). These results indicate that heterochromatin-lamina interactions can facilitate chromatin polymer phase separation and that heterochromatin self-affinity and lamina interactions can cooperatively increase nuclear fluctuations.

Increasing the heterochromatin-shell attraction affinity to large values (e.g., $u_{HS} > u_{HH}$) leads to the localization of all heterochromatin at the periphery, depleting heterochromatin from the nuclear interior (Figure C, D). Nevertheless, the uniformity of the peripheral facultative and constitutive heterochromatin phases is highly disrupted. In this case, constitutive heterochromatin is mixed with facultative heterochromatin due to the strong attraction of all heterochromatin with the shell overwhelming the self-affinity of different heterochromatin phases (snapshots on the right side of Figure 4C, D). Notably, the shape deviations from a sphere are elevated as the heterochromatin-shell interactions are further increased (Figure C,D).

However, in the case where heterochromatin-shell and heterochromatin-heterochromatin interactions are both strong, a new nuclear morphology emerges. Spherical domains of facultative heterochromatin at the periphery create chromatin-filled protrusions that bulge outward from the shell surface (Figure 4D, right column). While these structures are visually reminiscent of experimentally observed nuclear bleb[14,16,27,64], the simulated "blebs" are filled with heterochromatin, unlike the blebs observed in a variety of previous experiments, which generally contain less compact euchromatin[14,65–67]. Therefore, heterochromatin self-affinity and spatial distribution can alter nuclear morphology in our simulations. Furthermore, our model predicts a new polymer-physical mechanism through which bleb-like protrusions can be formed in cell nuclei with soft shells.

Nuclear Heterochromatin Content Affects Shell Morphology and Fluctuations

Studies show that decreasing decondensing chromatin, decreasing the overall level of heterochromatin or increasing the total amount of euchromatin is associated with abnormal nuclear morphology[14,27]. We therefore investigated whether the fraction of facultative heterochromatin per chromosome alters nuclear shape fluctuations in our model. To model these changes, we randomly convert euchromatin beads into facultative heterochromatin beads or vice versa. We vary the percentage of the chromatin fiber composed of facultative heterochromatin fraction from f=10% to f=75% (compared to our standard value of $f \approx 50\%$).

We find that increasing the facultative heterochromatin content elevates the nuclear shape fluctuations and introduces abnormalities in the morphology (Figure 5A). Up to f=55%, the primarily lower mode (larger lengthscale) fluctuations are elevated (Figure 5B). However, as the heterochromatin fraction increased toward f=75%, fluctuations increased across all wavenumbers. This manifested as a distorted nuclear morphology with wrinkles, bulges, and other features at various length scales (Figure 5C). The effect of higher facultative heterochromatin is enhanced at lower volume fractions and weakens as the volume fraction is increased (Figure 5B). Turning off the heterochromatin-shell attractive interactions (i.e., inverted nucleus) reduces the shape fluctuations for in the large f limit, suggesting that the observed effects are once again due to peripheral heterochromatin and its interactions with the lamina (SI text Figure S16-17 & S19).

Nevertheless, increasing heterochromatin levels in experiments generally leads to a more rounded nuclear shapes without nuclear blebs and shape disruption[14,27,68], which contradicts our simulation results (Figure 5C). We speculated that the combined effects of facultative heterochromatin self-attraction and attraction to the shell could be destabilizing nuclear shape in our simulations. We therefore repeated the high-heterochromatin simulations (f=75%) without heterochromatin self-affinity at the lowest volume fraction, where we observed the most drastic shape anomalies (φ=14%). Then, we observed that decreased shape fluctuations and less deformed morphologies (Figure 5D). However, as before (Figure 4), while weaker heterochromatin self-attractions decreased shape fluctuations, they also inhibited facultative heterochromatin phase separation in the nuclear interior and, albeit to a lesser extent, at the periphery (SI text Figure S11 & S12). Overall, our simulations showed that increasing the heterochromatin levels elevated nuclear shape fluctuations due to widespread distortions of the lamina via heterochromatin-lamina attractions, but heterochromatin decondensation was able to suppress this effect.

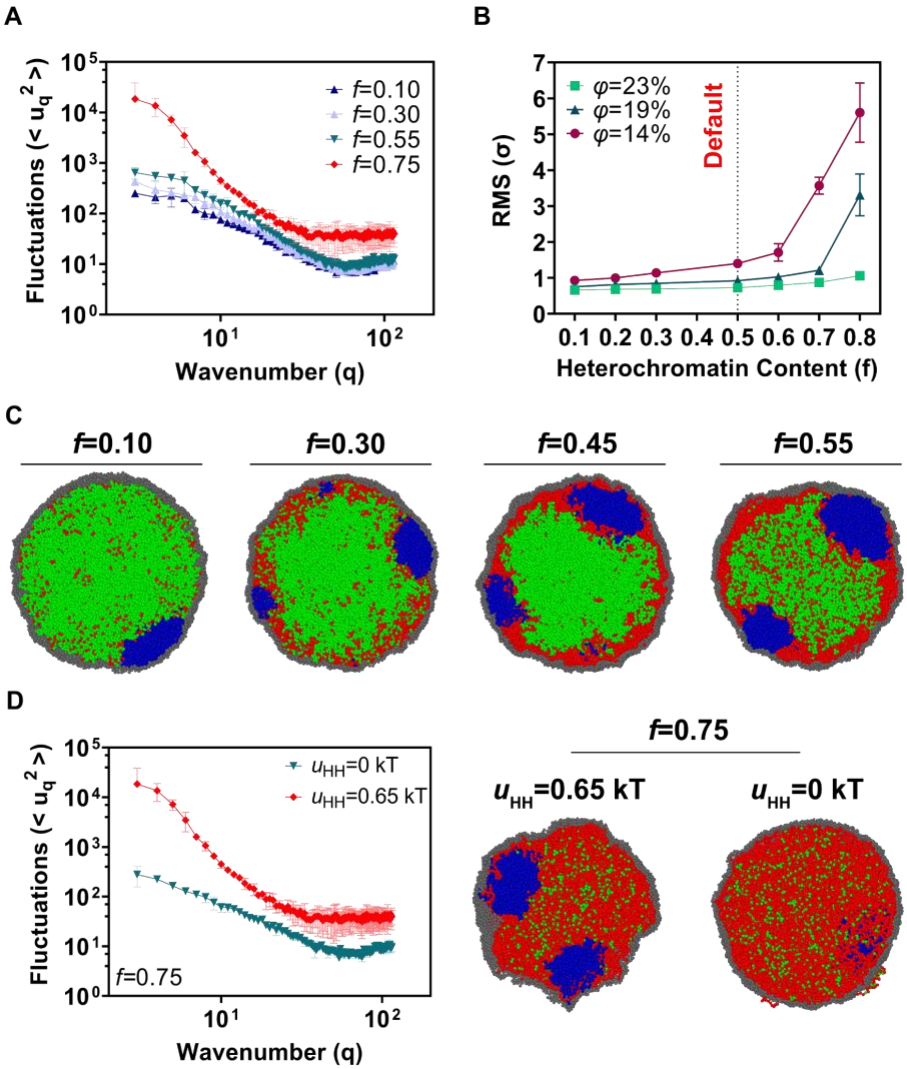

Figure 5) The facultative heterochromatin content at the nuclear periphery impacts the nuclear morphology. *A) Fourier spectra of shape fluctuations for conventional and inverted nuclei simulations, where the facultative heterochromatin content is set to f=10%, f=30%, f=45%, f=55%, and f=75%. The polymer volume fraction is set to φ=19%. B) RMS fluctuation amplitudes for varying levels of facultative heterochromatin at different volume fractions, with the value for standard simulations labeled as "default." C) Representative simulation snapshots for simulations with different levels of facultative heterochromatin. D) Shape fluctuations with and without heterochromatin self-affinity for f=75% case, along with simulation snapshots. Reducing self-affinity inhibits shape fluctuations in this scenario.*

Discussion

Using coarse-grained MD simulations, we modeled isolated cell nuclei encapsulating chromosomes to study the effects of heterochromatin organization on nuclear morphology. Chromosomes, which are composed of euchromatin and facultative and constitutive heterochromatin, were modeled as block copolymers containing three types of monomeric subunits[5]. We used an elastic shell model of the nuclear lamina to sterically confine the polymers within the nuclear volume[19,44,45]. Our model produces a broad spectrum of chromatin spatial distributions and nuclear shapes, depending on chromatin volume fraction, heterochromatin self-affinity and internal structure, heterochromatin-lamina interactions, and total heterochromatin content. We discuss these findings in detail below.

Chromatin volume fraction can repress nuclear shape fluctuations

Our simulations suggest that the volume fraction of the chromatin polymers can regulate the nuclear shape fluctuations and morphology. In particular, a higher volume fraction of chromatin supports a more regular nuclear shape (Figure 2), consistent with previous experiments and simulations in which chromatin was degraded (experiments) or not present (simulations) in the nucleus[44]. In our simulations, this is largely due to increased polymer osmotic pressure exerted outward on the nuclear lamina, which swells the nucleus and inhibits fluctuations. Consistently, in simulations higher in collapsed heterochromatin, polymer-based osmotic pressure (i.e., translational entropy) is limited, and shape fluctuations increase (Figure 4A-C, Figure 5). In our simulations, pressure due to the internal polymer is insufficient to generate localized nuclear deformations (i.e., blebs), but our observations are consistent with nuclear blebs *in vivo* generally contain transcriptionally-active euchromatin[14,65–67].

Experimentally, hyperosmotic osmotic pressures can lead to rapid chromatin collapse[57,69,70]. Although this condition corresponds to a shrinking nucleus and, thus, a higher chromatin mass density, chromatin itself collapses due to the change in salt conditions. This, in turn, reduces chromatin polymeric pressure. Consistently, hyperosmotic shock induces morphological distortions on the nuclear surface, similar to what we observe in our simulations with low chromatin volume fractions (Figure 2). Inversely, hypoosmotic shock leads to chromatin swelling, and consequently, more spherical nuclear shape[71], much as we observe in simulations with larger chromatin volume fractions. Therefore, we conclude that the effective volume fraction of chromatin within the nucleus can directly impact nuclear morphology.

Heterochromatin near the nuclear periphery can disrupt morphology of soft nuclei

Surprisingly, we found that compaction and overall levels of heterochromatin, particularly at the nuclear periphery, can drive large and widespread nuclear shape fluctuations across multiple lengthscales. This runs counter to experiments showing that high levels of heterochromatin[14,27], linkages within heterochromatin[32], and interactions between chromatin and the nuclear envelope all generally[13,40,41] stabilize cell nuclear shape.

Nonetheless, our simulations mirror findings in several specific scenarios with abnormal heterochromatin or lamina-associated proteins. In particular, in progeria patient cells bearing the lamin A/C mutation E145K, heterochromatin is enriched at regions of the nuclear envelope that exhibit large bleb-like protrusion[35]. These distorted regions are further notable for being depleted of lamin A/C, meaning that they are likely less stiff than the rest of the nuclear lamina[19,72–74]. Thus, the dense heterochromatin phase localized to the nuclear periphery may drive large nuclear shape aberrations in this scenario.

Our simulations predict that elevated binding of heterochromatin to the nuclear periphery can also promote nuclear morphological distortions. This contrasts with several experiments that depleted chromatin-binding proteins mediating interactions with the lamina[40,41,75]. Nonetheless, our simulations are consistent with other studies, such as a report in which cells inducibly expressing lamin A mutant progerin formed nuclear blebs and other abnormal nuclear morphologies[45]. Progerin-expressing cells also exhibited more frequent interactions between the lamina and polycomb heterochromatin. Corresponding simulations suggested that these interactions could be responsible for disrupting nuclear morphology. Beyond this study, our results also appear to be consistent with experiments in which lamin B receptor (LBR) is overexpressed and nuclei present abnormal morphologies[62,63]. Our simulations indicate that these experimental observations could be due to strong attractive interactions between heterochromatin and the nuclear lamina.

Such interactions can disrupt nuclear shape by bending the lamina to maximize interactions with the heterochromatin phase (Figure 4). Strong intra-heterochromatin interactions that compact heterochromatin could potentially amplify these effects (Figure 4). This would be especially notable in nuclei in which heterochromatin forms globular foci rather than a compact layer at the periphery. Further simulations showed that these effects are relatively weaker in simulations of stiffer nuclei (SI Figure S21), suggesting that heterochromatin phase separation could be disruptive particularly in nuclei or regions of nuclei that are more liquid-like or depleted of lamins. Thus, in some scenarios, heterochromatin compaction into mesoscale phases and heterochromatin-shell interactions could generate aberrant nuclear shape deformations.

Other possible mechanisms for regulation of nuclear shape by heterochromatin

To the extent that heterochromatin phase separation may enhance nuclear shape fluctuations and aberrations *in vivo*, our coarse-grained simulations suggest that the phase organization of heterochromatin does not generally stabilize the nuclear envelope against fluctuations. Therefore, the mechanistic question of how heterochromatin stabilizes cell nuclei against deformations, blebbing, and rupture remains open. Our simulations modeled an isolated nucleus with a relatively soft lamina in a quasi-equilibrium environment. Consequently, the simulated nuclei were not subject to external stresses due to intracellular and extracellular

forces. Various studies have indicated that interactions between the nucleus and the cytoskeleton can drive, and in some cases, suppress changes to nuclear morphology in a variety of scenarios[41,58,76–80]. In cases where heterochromatin or chromatin condensation inhibits alterations to nuclear shape[14,17,19,27,32,81,82], it may act by increasing nuclear stiffness to resist mechanical forces applied to the nucleus[19,32,82]. Beyond external driving, it remains unclear to what extent heterochromatin might stabilize nuclear morphology against internal perturbations, such as nonequilibrium driving by transcription and other motor activities[52,67]. Therefore, while chromatin condensation can have a disruptive effect on isolated nuclei, there are likely other mechanisms underpinning heterochromatin's effects on nuclear morphology *in vivo*.

Physical mechanism of heterochromatin-induced morphological fluctuations

In our simulations, increased heterochromatin compaction and levels increased nuclear morphological fluctuations (Figures 3 and 5). This effect may arise by one of several physical mechanisms. Increasing the amount of heterochromatin or its self-affinity increases the amount of collapsed polymer in our simulations. In polymer physical terms, increasing heterochromatin increases the amount of polymer in poor solvent conditions. This generates a lower polymeric pressure inside the nucleus, which allows the lamina, a polymeric shell (or solid membrane) to fluctuate and distort. Consistently, simulations without heterochromatin self-affinity leads to smaller shape fluctuations due to increased polymeric pressure (which is due to increased translational entropy of heterochromatic regions), even at the highest levels of heterochromatin (Figure 5D). These observations parallel the changes in nuclear morphology that we observe when decreasing the chromatin polymer volume fraction (Figure 2).

Complementarily, polymer self-affinity combined with attractive interactions to a peripheral boundary can physically deform the boundary to lower the free energy of the system. Experiments with proteins condensing within lipid vesicles[83] showed that strong phase separation can lead to the formation of long protein-coated lipid tubules and other structures. Similarly, theoretical modeling has indicated that phase condensation on a biopolymeric surface can generate morphological deformations on the surface[84]. More broadly, several experiments have recently demonstrated that biological phase separation can induce forces on substrates ranging from single-molecule DNA to chromatin[85–87].

Furthermore, we note that while regular copolymers (i.e., with well-defined blocks) are known to undergo microscopic phase separation and exhibit highly regular phase[88], random copolymers can form heterogeneous local domains[89]. However, the mechanisms explored by our simulations require nuclear-scale alterations to heterochromatin phase organization to generate nuclear-scale shape aberrations. We observed that this may occur by small localized domains merging with larger mesoscopic domains near the periphery. This increases the nonuniformity of chromatin organization at the nuclear periphery, which

facilitates larger effects on nuclear shape. Thus, epigenetic changes that promote large-scale phase formations at specific peripheral sites are most likely to disrupt nuclear shape.

In summary, our model suggests that chromatin organization, via chromatin volume density and heterochromatic phase separation, can alter nuclear morphology. Strikingly, heterochromatin phase separation, especially at the nuclear periphery, *promotes* disruption of nuclear shape. Since heterochromatin is generally considered to stabilize nuclear shape, our simulations suggest that the architectural effects of heterochromatin phase separation must be balanced by other aspects of nuclear mechanical response and organization. However, our model predicts that in nuclei with soft laminas or excessive heterochromatin recruitment to the nuclear lamina, this balance may be disrupted. Therefore, our simulations predict a new, largely unappreciated mechanism by which chromatin may regulate nuclear morphology.

Acknowledgements

We thank Martin Falk for instructive discussions. EJB thanks Andrew Stephens and John F. Marko for helpful discussions. EJB acknowledges support from the NIH Common Fund 4D Nucleome Program (UM1HG011536). AE acknowledges the National Science Center, Poland (Grant Polonez Bis No.~2021/43/P/ST3/01833). AGA and AE acknowledge TUBITAK, The Scientific and Technological Research Council of Turkey (1001 Grant No. 122F309)

Bibliography

1. Mirny, L. A., Imakaev, M. & Abdennur, N. Two major mechanisms of chromosome organization. *Curr. Opin. Cell Biol.* 58, 142–152 (2019).
2. Jost, D., Carrivain, P., Cavalli, G. & Vaillant, C. Modeling epigenome folding: formation and dynamics of topologically associated chromatin domains. *Nucleic Acids Res.* 42, 9553–9561 (2014).
3. Bajpai, G., Amiad Pavlov, D., Lorber, D., Volk, T. & Safran, S. Mesoscale phase separation of chromatin in the nucleus. *eLife* 10, e63976 (2021).
4. Amiad-Pavlov, D. *et al.* Live imaging of chromatin distribution reveals novel principles of

nuclear architecture and chromatin compartmentalization. *Sci. Adv.* 7, eabf6251 (2021).

5. Falk, M. *et al.* Heterochromatin drives compartmentalization of inverted and conventional nuclei. *Nature* 570, 395–399 (2019).
6. Gorkin, D. U., Leung, D. & Ren, B. The 3D Genome in Transcriptional Regulation and Pluripotency. *Cell Stem Cell* 14, 762–775 (2014).
7. Zheng, H. & Xie, W. The role of 3D genome organization in development and cell differentiation. *Nat. Rev. Mol. Cell Biol.* 20, 535–550 (2019).
8. Bonev, B. & Cavalli, G. Organization and function of the 3D genome. *Nat. Rev. Genet.* 17, 661–678 (2016).
9. Kubben, N. *et al.* Mapping of lamin A- and progerin-interacting genome regions. *Chromosoma* 121, 447–464 (2012).
10. San Martin, R. *et al.* Chromosome compartmentalization alterations in prostate cancer cell lines model disease progression. *J. Cell Biol.* 221, e202104108 (2021).
11. Zhou, Y. *et al.* Temporal dynamic reorganization of 3D chromatin architecture in hormone-induced breast cancer and endocrine resistance. *Nat. Commun.* 10, 1522 (2019).
12. Barutcu, A. R. *et al.* Chromatin interaction analysis reveals changes in small chromosome and telomere clustering between epithelial and breast cancer cells. *Genome Biol.* 16, 214 (2015).
13. Stephens, A. D., Banigan, E. J. & Marko, J. F. Chromatin's physical properties shape the nucleus and its functions. *Curr. Opin. Cell Biol.* 58, 76–84 (2019).
14. Stephens, A. D. *et al.* Chromatin histone modifications and rigidity affect nuclear morphology independent of lamins. *Mol. Biol. Cell* 29, 220–233 (2018).
15. Samwer, M. *et al.* DNA Cross-Bridging Shapes a Single Nucleus from a Set of Mitotic

Chromosomes. *Cell* 170, 956-972.e23 (2017).

16. Furusawa, T. *et al.* Chromatin decompaction by the nucleosomal binding protein HMGN5 impairs nuclear sturdiness. *Nat. Commun.* 6, 6138 (2015).
17. Wang, P. *et al.* WDR5 modulates cell motility and morphology and controls nuclear changes induced by a 3D environment. *Proc. Natl. Acad. Sci.* 115, 8581–8586 (2018).
18. Solovei, I. *et al.* Nuclear Architecture of Rod Photoreceptor Cells Adapts to Vision in Mammalian Evolution. *Cell* 137, 356–368 (2009).
19. Stephens, A. D., Banigan, E. J., Adam, S. A., Goldman, R. D. & Marko, J. F. Chromatin and lamin A determine two different mechanical response regimes of the cell nucleus. *Mol. Biol. Cell* 28, 1984–1996 (2017).
20. Shimamoto, Y., Tamura, S., Masumoto, H. & Maeshima, K. Nucleosome–nucleosome interactions via histone tails and linker DNA regulate nuclear rigidity. *Mol. Biol. Cell* 28, 1580–1589 (2017).
21. Ghosh, S., Cuevas, V. C., Seelbinder, B. & Neu, C. P. Image-Based Elastography of Heterochromatin and Euchromatin Domains in the Deforming Cell Nucleus. *Small Weinh. Bergstr. Ger.* 17, e2006109 (2021).
22. Brunet, A., Destainville, N. & Collas, P. Physical constraints in polymer modeling of chromatin associations with the nuclear periphery at kilobase scale. *Nucleus* 12, 6–20 (2021).
23. Girard, M., Cruz, M. O. de la, Marko, J. F. & Erbaş, A. Heterochromatin flexibility contributes to chromosome segregation in the cell nucleus. 2020.12.01.403832 Preprint at https://doi.org/10.1101/2020.12.01.403832 (2020).
24. Cook, P. R. & Marenduzzo, D. Entropic organization of interphase chromosomes. *J. Cell Biol.* 186, 825–834 (2009).

25. Di Stefano, M., Nützmann, H.-W., Marti-Renom, M. A. & Jost, D. Polymer modelling unveils the roles of heterochromatin and nucleolar organizing regions in shaping 3D genome organization in *Arabidopsis thaliana*. *Nucleic Acids Res.* 49, 1840–1858 (2021).
26. Xia, Y. *et al.* Nuclear rupture at sites of high curvature compromises retention of DNA repair factors. *J. Cell Biol.* 217, 3796–3808 (2018).
27. Stephens, A. D. *et al.* Physicochemical mechanotransduction alters nuclear shape and mechanics via heterochromatin formation. *Mol. Biol. Cell* 30, 2320–2330 (2019).
28. Butin-Israeli, V., Adam, S. A., Goldman, A. E. & Goldman, R. D. Nuclear lamin functions and disease. *Trends Genet.* 28, 464–471 (2012).
29. Kalukula, Y., Stephens, A. D., Lammerding, J. & Gabriele, S. Mechanics and functional consequences of nuclear deformations. *Nat. Rev. Mol. Cell Biol.* 23, 583–602 (2022).
30. Strom, A. R. *et al.* Phase separation drives heterochromatin domain formation. *Nature* 547, 241–245 (2017).
31. Larson, A. G. *et al.* Liquid droplet formation by HP1α suggests a role for phase separation in heterochromatin. *Nature* 547, 236–240 (2017).
32. Strom, A. R. *et al.* HP1α is a chromatin crosslinker that controls nuclear and mitotic chromosome mechanics. *eLife* 10, e63972 (2021).
33. Solovei, I. *et al.* LBR and Lamin A/C Sequentially Tether Peripheral Heterochromatin and Inversely Regulate Differentiation. *Cell* 152, 584–598 (2013).
34. Goldman, R. D. *et al.* Accumulation of mutant lamin A causes progressive changes in nuclear architecture in Hutchinson–Gilford progeria syndrome. *Proc. Natl. Acad. Sci.* 101, 8963–8968 (2004).
35. Taimen, P. *et al.* A progeria mutation reveals functions for lamin A in nuclear assembly,

architecture, and chromosome organization. *Proc. Natl. Acad. Sci. U. S. A.* 106, 20788–20793 (2009).

36. Haithcock, E. *et al.* Age-related changes of nuclear architecture in Caenorhabditis elegans. *Proc. Natl. Acad. Sci.* 102, 16690–16695 (2005).
37. Hoskins, V. E., Smith, K. & Reddy, K. L. The Shifting Shape of Genomes: Dynamics of Heterochromatin Interactions at the Nuclear Lamina. *Curr. Opin. Genet. Dev.* 67, 163–173 (2021).
38. Harr, J. C. *et al.* Directed targeting of chromatin to the nuclear lamina is mediated by chromatin state and A-type lamins. *J. Cell Biol.* 208, 33–52 (2015).
39. Zheng, X. *et al.* Lamins Organize the Global Three-Dimensional Genome from the Nuclear Periphery. *Mol. Cell* 71, 802-815.e7 (2018).
40. Poleshko, A. *et al.* The Human Protein PRR14 Tethers Heterochromatin to the Nuclear Lamina During Interphase and Mitotic Exit. *Cell Rep.* 5, 10.1016/j.celrep.2013.09.024 (2013).
41. Schreiner, S. M., Koo, P. K., Zhao, Y., Mochrie, S. G. J. & King, M. C. The tethering of chromatin to the nuclear envelope supports nuclear mechanics. *Nat. Commun.* 6, 7159 (2015).
42. Brahmachari, S., Contessoto, V. G., Di Pierro, M. & Onuchic, J. N. Shaping the genome via lengthwise compaction, phase separation, and lamina adhesion. *Nucleic Acids Res.* 50, 4258–4271 (2022).
43. Laghmach, R., Di Pierro, M. & Potoyan, D. A. The interplay of chromatin phase separation and lamina interactions in nuclear organization. *Biophys. J.* 120, 5005–5017 (2021).
44. Banigan, E. J., Stephens, A. D. & Marko, J. F. Mechanics and Buckling of Biopolymeric

Shells and Cell Nuclei. *Biophys. J.* 113, 1654–1663 (2017).

45. Lionetti, M. C. *et al.* Chromatin and Cytoskeletal Tethering Determine Nuclear Morphology in Progerin-Expressing Cells. *Biophys. J.* 118, 2319–2332 (2020).
46. Kremer, K. & Grest, G. S. Dynamics of entangled linear polymer melts: A molecular-dynamics simulation. *J. Chem. Phys.* 92, 5057–5086 (1990).
47. Dekker, J. & Mirny, L. The 3D Genome as Moderator of Chromosomal Communication. *Cell* 164, 1110–1121 (2016).
48. McCord, R. P., Kaplan, N. & Giorgetti, L. Chromosome Conformation Capture and Beyond: Toward an Integrative View of Chromosome Structure and Function. *Mol. Cell* 77, 688–708 (2020).
49. Rao, S. S. P. *et al.* A 3D Map of the Human Genome at Kilobase Resolution Reveals Principles of Chromatin Looping. *Cell* 159, 1665–1680 (2014).
50. Rosa, A. & Everaers, R. Structure and Dynamics of Interphase Chromosomes. *PLoS Comput. Biol.* 4, e1000153 (2008).
51. Plimpton, S. Fast Parallel Algorithms for Short-Range Molecular Dynamics. *J. Comput. Phys.* 117, 1–19 (1995).
52. Liu, K., Patteson, A. E., Banigan, E. J. & Schwarz, J. M. Dynamic Nuclear Structure Emerges from Chromatin Cross-Links and Motors. *Phys. Rev. Lett.* 126, 158101 (2021).
53. Biswas, A. *et al.* Conserved nucleocytoplasmic density homeostasis drives cellular organization across eukaryotes. 2023.09.05.556409 Preprint at https://doi.org/10.1101/2023.09.05.556409 (2023).
54. Mazumder, A., Roopa, T., Basu, A., Mahadevan, L. & Shivashankar, G. V. Dynamics of Chromatin Decondensation Reveals the Structural Integrity of a Mechanically Prestressed

Nucleus. *Biophys. J.* 95, 3028–3035 (2008).

55. Neubert, E. *et al.* Chromatin swelling drives neutrophil extracellular trap release. *Nat. Commun.* 9, 3767 (2018).
56. Kim, K. & Guck, J. The Relative Densities of Cytoplasm and Nuclear Compartments Are Robust against Strong Perturbation. *Biophys. J.* 119, 1946–1957 (2020).
57. Olins, A. L., Gould, T. J., Boyd, L., Sarg, B. & Olins, D. E. Hyperosmotic stress: in situ chromatin phase separation. *Nucleus* 11, 1–18 (2020).
58. Chu, F.-Y., Haley, S. C. & Zidovska, A. On the origin of shape fluctuations of the cell nucleus. *Proc. Natl. Acad. Sci.* 114, 10338–10343 (2017).
59. Kiseleva, A. A., Cheng, Y.-C., Smith, C. L., Katz, R. A. & Poleshko, A. PRR14 organizes H3K9me3-modified heterochromatin at the nuclear lamina. *Nucleus* 14, 2165602 (2023).
60. Poleshko, A. *et al.* H3K9me2 orchestrates inheritance of spatial positioning of peripheral heterochromatin through mitosis. *eLife* 8, e49278.
61. Lammerding, J. *et al.* Abnormal nuclear shape and impaired mechanotransduction in emerin-deficient cells. *J. Cell Biol.* 170, 781–791 (2005).
62. Carvajal, A. S., McKenna, T., Arzt, E. W. & Eriksson, M. Overexpression of Lamin B Receptor Results in Impaired Skin Differentiation. *PLOS ONE* 10, e0128917 (2015).
63. Olins, A. L., Rhodes, G., Welch, D. B. M., Zwerger, M. & Olins, D. E. Lamin B receptor. *Nucleus* 1, 53–70 (2010).
64. Lammerding, J. *et al.* Lamins A and C but Not Lamin B1 Regulate Nuclear Mechanics*. *J. Biol. Chem.* 281, 25768–25780 (2006).
65. Shimi, T. *et al.* The A- and B-type nuclear lamin networks: microdomains involved in chromatin organization and transcription. *Genes Dev.* 22, 3409–3421 (2008).

66. Bercht Pfleghaar, K. *et al.* Gene-rich chromosomal regions are preferentially localized in the lamin B deficient nuclear blebs of atypical progeria cells. *Nucleus* 6, 66–76 (2015).

67. Berg, I. K. *et al.* Transcription inhibition suppresses nuclear blebbing and rupture independent of nuclear rigidity. *J. Cell Sci.* jcs.261547 (2023) doi:10.1242/jcs.261547.

68. Nava, M. M. *et al.* Heterochromatin-Driven Nuclear Softening Protects the Genome against Mechanical Stress-Induced Damage. *Cell* 181, 800-817.e22 (2020).

69. Finan, J. D., Leddy, H. A. & Guilak, F. Osmotic stress alters chromatin condensation and nucleocytoplasmic transport. *Biochem. Biophys. Res. Commun.* 408, 230–235 (2011).

70. Khavari, A. & Ehrlicher, A. J. Nuclei deformation reveals pressure distributions in 3D cell clusters. *PLOS ONE* 14, e0221753 (2019).

71. Finan, J. D., Chalut, K. J., Wax, A. & Guilak, F. Nonlinear Osmotic Properties of the Cell Nucleus. *Ann. Biomed. Eng.* 37, 477–491 (2009).

72. Swift, J. *et al.* Nuclear Lamin-A Scales with Tissue Stiffness and Enhances Matrix-Directed Differentiation. *Science* 341, 1240104 (2013).

73. Pajerowski, J. D., Dahl, K. N., Zhong, F. L., Sammak, P. J. & Discher, D. E. Physical plasticity of the nucleus in stem cell differentiation. *Proc. Natl. Acad. Sci.* 104, 15619–15624 (2007).

74. Lammerding, J. *et al.* Lamin A/C deficiency causes defective nuclear mechanics and mechanotransduction. *J. Clin. Invest.* 113, 370–378 (2004).

75. Mattout, A. *et al.* An EDMD Mutation in C. elegans Lamin Blocks Muscle-Specific Gene Relocation and Compromises Muscle Integrity. *Curr. Biol.* 21, 1603–1614 (2011).

76. Larrieu, D., Britton, S., Demir, M., Rodriguez, R. & Jackson, S. P. Chemical Inhibition of NAT10 Corrects Defects of Laminopathic Cells. *Science* 344, 527–532 (2014).

77. Hatch, E. M. & Hetzer, M. W. Nuclear envelope rupture is induced by actin-based nucleus confinement. *J. Cell Biol.* 215, 27–36 (2016).

78. Mistriotis, P. *et al.* Confinement hinders motility by inducing RhoA-mediated nuclear influx, volume expansion, and blebbing. *J. Cell Biol.* 218, 4093–4111 (2019).

79. Patteson, A. E. *et al.* Vimentin protects cells against nuclear rupture and DNA damage during migration. *J. Cell Biol.* 218, 4079–4092 (2019).

80. Pho, M. *et al.* Actin contraction controls nuclear blebbing and rupture independent of actin confinement. 2022.12.01.518663 Preprint at https://doi.org/10.1101/2022.12.01.518663 (2022).

81. Hobson, C. M. *et al.* Correlating nuclear morphology and external force with combined atomic force microscopy and light sheet imaging separates roles of chromatin and lamin A/C in nuclear mechanics. *Mol. Biol. Cell* 31, 1788–1801 (2020).

82. Chalut, K. J. *et al.* Chromatin Decondensation and Nuclear Softening Accompany Nanog Downregulation in Embryonic Stem Cells. *Biophys. J.* 103, 2060–2070 (2012).

83. Yuan, F. *et al.* Membrane bending by protein phase separation. *Proc. Natl. Acad. Sci.* 118, e2017435118 (2021).

84. Bergeron-Sandoval, L.-P. & Michnick, S. W. Mechanics, Structure and Function of Biopolymer Condensates. *J. Mol. Biol.* 430, 4754–4761 (2018).

85. Quail, T. *et al.* Force generation by protein–DNA co-condensation. *Nat. Phys.* 17, 1007–1012 (2021).

86. Strom, A. R. *et al.* Condensate-driven interfacial forces reposition DNA loci and measure chromatin viscoelasticity. 2023.02.27.530281 Preprint at https://doi.org/10.1101/2023.02.27.530281 (2023).

87. Shin, Y. *et al.* Liquid Nuclear Condensates Mechanically Sense and Restructure the Genome. *Cell* 175, 1481-1491.e13 (2018).

88. Leibler, L. Theory of Microphase Separation in Block Copolymers. *Macromolecules* 13, 1602–1617 (1980).

89. B. W. Swift & M. Olvera de la Cruz. Random copolymers in concentrated solutions. *Europhys. Lett.* 35, 487 (1996).